

miR-146a is a pivotal regulator of neutrophil extracellular trap formation promoting thrombosis

Ana B. Arroyo,^{1*} María P. Fernández-Pérez,^{1*} Alberto del Monte,^{2*} Sonia Águila,¹ Raúl Méndez,³ Rebecca Hernández-Andolín,¹ Nuria García-Barberá,¹ Ascensión M. de los Reyes-García,¹ Paula González-Jiménez,³ María I. Arcas,⁴ Vicente Vicente,^{1,5} Rosario Menéndez,^{3,6} Vicente Andrés,^{2,7} Rocío González-Conejero^{1#} and Constantino Martínez^{1#}

¹Department of Hematology and Medical Oncology, Morales Meseguer University Hospital, Centro Regional de Hemodonación, Universidad de Murcia, IMIB-Arixaca, Murcia; ²Centro Nacional de Investigaciones Cardiovasculares Carlos III (CNIC), Madrid; ³Servicio de Neumología, Hospital Universitario y Politécnico La Fe/Instituto de Investigación Sanitaria (IIS) La Fe, La Fe; ⁴Department of Pathology, Hospital Reina Sofía, Murcia; ⁵CIBER de Enfermedades raras (CIBER-ER), Murcia; ⁶Centro de Investigación en Red en Enfermedades Respiratorias (CIBER-ES, CB06/O6/0028), Madrid and ⁷CIBER de Enfermedades Cardiovasculares (CIBER-CV), Madrid, Spain.

*ABA, MPF-P, and AdM contributed equally as co-first authors.

#RG-C and CM contributed equally as co-senior authors.

©2021 Ferrata Storti Foundation. This is an open-access paper. doi:10.3324/haematol.2019.240226

Received: November 5, 2019.

Accepted: June 19, 2020.

Pre-published: June 25, 2020.

Correspondence: ROCÍO GONZÁLEZ-CONEJERO - rocio.gonzalez@carm.es, constant@um.es

miR-146a is a pivotal regulator of neutrophil extracellular trap formation promoting thrombosis

Arroyo AB et al.

Supplemental Material

Mice

Animal welfare, experimental and other scientific procedures with animals conformed to EU Directive 2010/63EU and Recommendation 2007/526/EC, enforced in Spanish law under Real Decreto 53/2013. Moreover, the animal research included in this work was granted a formal ethics approval by the Committees in charge of animal welfare at Centro Nacional de Investigaciones Cardiovasculares Carlos III (OEBA-CNIC) and Universidad de Murcia (CEEA-UM). The ethics approval numbers from the legally competent authorities are PROEX 134/14 (CAM) and A13150602 (DAW-RM). Ldl receptor-deficient mice (*Ldlr*^{-/-}) (Charles River Laboratories), miR-146a deficient mice [*miR-146a*^{-/-} (stock# 016239)] were backcrossed for more than 8 generations in a C57BL/6J CD45.2 background (The Jackson Laboratory, Bar Harbor, ME) and inbred wild-type (WT) littermates were maintained under controlled environmental conditions (relative humidity: 45-65%; temperature: 20-24°C) with a 12h light/dark cycle and free access to chow and water. All mice used in this study were 8-12 weeks old and indistinctly male and female were included.

Endotexemia model

Peripheral blood was collected in 3.2% citrate at 0, 4 and 24h after LPS injection by retro-orbital bleeding. Circulating blood cells were quantified using the PENTRA 80 hematology platform (HORIBA Medical, Madrid, Spain). Glass slides were stained for reticulin automatically in the pathologic anatomy service from Morales Meseguer Hospital (Murcia, Spain). The histological index of lung injury included reticulin deposition, fibers thickening, and leukocyte infiltration. The images were scanned automatically using a Leica SCN400F microscope (Leica Biosystems, L'hospitalet de Llobregat, Spain).

Plasma measurement

Platelet-poor plasma (PPP) from mice was isolated by centrifugation of whole blood (1500g x 5 min at RT). Aliquots were stored at -80°C to allow batch analysis. Cell free DNA (cfDNA) are fragments of double-stranded DNA with variable molecular weight, including short fragments (70–200 bp) or long fragments up to 21 kb. cfDNA is released into the plasma by different

physiologic and pathologic mechanisms, by apoptotic and necrotic cells. But not all cfDNA comes from cell death. Excessive NET formation and the insufficient clearance of NETs also result in an increase in the levels of circulating cfDNA. Thus, cfDNA was quantified by fluorescence using 1 μ M Sytox[®] Green reagent (ThermoFisher, Madrid, Spain). Commercial DNA from salmon sperm (Sigma-Aldrich, Madrid, Spain) was used to generate the standard curve for Sytox measurements. Plasma samples (10 μ l) were assayed in triplicate. After incubation (15 min in dark) fluorescence was read at 488 nm in a microplate reader (Biotek[®] Sinergy TM Ht, Winooski, VT).

For western blot assays, plasma samples (1 μ L) were separated by SDS-PAGE (15%) in reducing conditions. Gels were transferred onto PVDF membranes (Amersham Hybond P 0.45, GE Healthcare, Barcelona, Spain) and blocked for 1h in 2% w/v BSA-PBS. Antibody against citH3 (anti-histone H3 citrulline R2+R8+R17 antibody, Abcam, Madrid, Spain) was diluted 1:1000 and incubated overnight at 4°C. After washing, membranes were incubated with anti-rabbit secondary antibody labeled with peroxidase (1:10000, GE Healthcare, Barcelona, Spain) for 1h at RT. ECL Prime Detection Kit and ImageQuant LAS 4000 Imager (GE Healthcare, Barcelona, Spain) were used for protein detection. Densitometric analyses were performed with ImageJ software ¹.

ROS were analyzed using the *OxiSelect[™] in vitro ROS/RNS assay kit* (STA-347, Cell Biolabs, Bionova, Madrid, Spain). Thrombin-antithrombin complexes (TAT) were quantified using the commercial *TAT Complexes Mouse ELISA kit ab137994* (Abcam, Madrid, Spain). NE was measured using the *Mouse Elastase 2, Neutrophil (Ela2) Enzyme-linked Immunosorbent Assay Kit* (Cloud-clone corporation, Madrid, Spain). In each case, we followed the manufacturer's protocol.

Immunofluorescence on tissue sections

4 μ m tissue sections that were mounted, dried on Superfrost Ultra Plus slides (ThermoFisher Scientific, Madrid, Spain), dewaxed and rehydrated. Antigen retrieval of aortic valves was performed in R-Universal buffer at 50°C for 90 min (Aptum biologics, Southampton, UK). Sections were permeabilized for 5 min with 0.5% Triton X100 in TBS at RT. Sections were treated with blocking buffer [TBS supplemented with 1% bovine serum albumin (BSA), 2% goat normal serum (Abcam, Madrid, Spain), 5% cold water fish gelatin (Sigma Aldrich, Madrid, Spain), 0.05% Tween-20, 0.05% Triton-X100] for 1h at RT. Samples were incubated with primary antibodies diluted in blocking buffer at RT overnight [1:50 Chicken anti-histone H2B (Abcam, Madrid, Spain), and 1:50 rabbit anti-neutrophil elastase (NE) (Merck Millipore, Madrid, Spain)]. Secondary antibodies [goat anti-rabbit Alexa Fluor 488, and goat anti-chicken Alexa Fluor 633 (ThermoFisher Scientific, Madrid, Spain)] diluted 1:500 in

blocking buffer were incubated for 1h at RT. Samples were air dried and mounted with ProLong Gold with DAPI (ThermoFisher Scientific, Madrid, Spain).

Antigen retrieval of carotid artery sections was performed by incubation in citrate buffer pH6 for 20 min at 96°C. After antigen retrieval, sections blocked with BSA 5% in PBS for 1h at RT. After blocking, samples were rinsed twice with PBT (PBS-0.05% Tween-20) and incubated overnight at 4°C with rabbit anti-citH3 (R2+R8+R17; Abcam, Madrid, Spain) diluted 1:50 in PBS with 1% BSA. After rinsing, samples were incubated with goat anti-rabbit Alexa Fluor 488 (ThermoFisher Scientific, Madrid, Spain) diluted 1:500 in PBS with 1% BSA for 1h at RT. Preparations were visualized, and images were captured in a Leica SP8 Confocal Microscope (Leica Biosystems, L' Hospitalet de Llobregat, Spain). High resolution image montages (63X) of whole aortic valves and carotid sections were obtained by using Tile Scan LAS AF tool. Images were processed and digitally merged with Fiji processing package². Due to technical issues, we used two different approaches to visualize NETs. In the atherosclerosis model, we stained the aortic roots with NE, DAPI, and H2B using R-Universal buffer at 50°C as antigen retrieval method following the recommendations for NET identification given by Brinkmann et al³. However, this same protocol in the carotid thrombi did not succeed. To allow the antibodies access into the thrombus, it was necessary to perform heat induced antigen retrieval (96°C, 20 min) in citrate buffer pH6. Since NE staining is lost at 96°C³, we alternatively used citH3 as a well characterized NET-specific antigen.

Analysis for aortic valves

Quantification analysis for H2B and NE in aortic valves sections was performed with Colocalization Colormap Fiji plugin. This software calculates index of correlation (ICorr) that represents the fraction of positively correlated (colocalized) pixels in the analyzed images. In addition, Coloc 2 Fiji plugin, which implements and performs the pixel intensity correlation through Pearson and Costes methods, was used to compare the distributions of fluorescence intensities of H2B and NE signals in a region of interest (ROI).

Quantification of total and citrullinated H3 positive cells in carotid sections

Total infiltrated nucleated cells and citH3 positive cells in the thrombi and the adventitial layer of carotid sections were counted and scored in a blinded fashion by 2 observers by using the Cell Counter Fiji's plugin. Intraclass correlation coefficient (ICC) was used to assess the agreement of the two observers.

Flow cytometry

250 µL of whole blood from mice was drawn on 10% citrate. Briefly, 50 µL of blood was incubated with 50 µL of PBE (0.5% p/v BSA and 2 mM EDTA in PBS) containing 1 µL of

Alexa Fluor 647 anti-mouse Ly6G antibody, 1 μ L of PerCP/Cy5.5 anti-mouse CD62L Antibody, 2 μ L of Brilliant Violet 421 anti-mouse CD184 (Cxcr4) (Biolegend, San Diego, CA), 2 μ L of PE anti-mouse CD181 (Cxcr1) antibody (BD Pharmingen, Madrid, Spain), 1 μ L of PE anti-mouse CD11b (Thermo Fisher Scientific, Waltham, MA, USA) or 2 μ L PE anti-mouse Tlr4 antibody (Biolegend) for 25 min at RT. Then, 1 mL of Lysing Solution 1X (BD Biosciences, Madrid, Spain) was added and incubated for 5 min at RT to remove red blood cells. Finally, cells were centrifuged at 400xg for 5 min and resuspended in 350 μ L of PBE. CD11b, CD62L and Cxcr1 levels were determined on Ly6G-positive neutrophils by using a BD Accury C6 Flow Cytometer (BD Biosciences, San Jose, CA, USA). Cxcr4 and Tlr4 were analyzed by using a LSRFortessa™ X-20 cell analyzer (BD Biosciences, San Jose, CA). Data were analyzed using FlowJo cell analysis software (FlowJo, LLC, Ashland, OR).

For basal ROS measurement, bone marrow (BM) neutrophils from WT and *miR-146a*^{-/-} mice were isolated by negative immune selection (Neutrophil Isolation kit, Miltenyi Biotec, Madrid, Spain). Neutrophils were incubated with 10 μ M 2',7'-dichlorodihydrofluorescein diacetate (H2DCFDA) (ThermoFisher, Madrid, Spain) at 37°C for 30 min and then washed with Hank's buffer (Thermofisher Scientific, Madrid, Spain). 7-aminoactinomycin D staining was used to exclude death cells for the analysis. Samples were analyzed in the BD Accury C6 Flow Cytometer.

Oxygen consumption rate analysis

BM neutrophils from WT and *miR-146a*^{-/-} mice were isolated and seeded on Corning Cell-Tak™ (Fisher Scientific, Madrid, Spain) coated Seahorse culture microplate at a density of 1 x 10⁵ cells and centrifuged at 300 x g 2 min with no brake. Wells were gently filled with Seahorse media and plate was incubated at 37°C without CO₂ for 50 min. Basal oxygen consumption rate (OCR) was measured using a Seahorse XFe96 Analyzer (Agilent Technologies, Madrid, Spain).

Patients

The inclusion criteria were: diagnosis of pneumonia based on a new radiological infiltrate with at least two compatible clinical symptoms, age 18-85 years, microbiological diagnosis confirmed, and Pneumonia Severity Index (PSI) > II⁴. Exclusion criteria were: admission in the previous 15 days, residence in a nursing home, immunosuppressive treatments and human immunodeficiency virus (HIV) +. All patients who met eligibility criteria or next kin provided written informed consent. Collected data were age, gender, smoking habit, vaccination status, comorbidities, analytical results at admission and prior treatments. Initial severity was assessed by PSI, CURB65, sepsis status⁵ and Sequential Organ Failure Assessment (SOFA) score⁶. The outcome considered were clinical stability, length of stay (LOS), cardiovascular events,

mortality (in-hospital and 30-day), and treatment failure. Clinical stability was defined using the modified Halm criteria ⁷. Treatment failure was defined as previously described ⁸ and included early and late failures. Early treatment failure was defined as clinical deterioration within 72h of treatment, as indicated by the need for mechanical ventilation and/or shock, or death. Late treatment failure was defined as persistence or reappearance of fever (>37.8°C), radiographic progression (>50% increase), including pleural effusion and/or empyema, nosocomial infection, impairment of respiratory failure (defined as PO₂/FiO₂ <250 with respiratory rate ≥30/min) and need for mechanical ventilation or shock after 72h. The occurrence of cardiovascular events was considered if any of the following appeared during hospitalization: acute coronary syndrome (AMI or unstable angina), new or worsening heart failure, *de novo* or recurrent arrhythmia requiring hospital admission or emergency department care, cerebrovascular accident (stroke or transient ischemic attack), and/or venous thromboembolic disease (deep venous thrombosis of the leg or pulmonary embolism) ⁹. Among 18 patients with cardiovascular event or treatment failure (Supplemental Table S2), 6 patients had only cardiovascular events, 9 patients had only treatment failure, and 3 had both cardiovascular events and treatment failure. Patients with cardiovascular complications (6 with cardiovascular events and 3 with cardiovascular events/treatment failure) suffered from 11 events as follows: 3 arrhythmias, 3 heart failures, 1 stroke, 1 myocardial infarction/arrhythmia and 1 heart failure/arrhythmia.

Blood samples from patients were collected in EDTA at day 1 from entry. Plasmas were isolated by centrifugation (2000xg10 min at RT). Aliquots were stored at -80°C to allow batch analysis. DNA was extracted from the buffy coat by using QIAamp® DNA Blood Mini Kit (Qiagen, Madrid, Spain) automatically (QIAcube, Qiagen).

Genotyping

Rs2431697 of *MIR146A* was genotyped using TaqMan® SNP Genotyping Assays C_26693319_10 (ThermoFisher, Madrid, Spain) according to the manufacturer's recommendation. All genotypes were confirmed by sequencing of randomly selected samples.

DNA-citH3 ELISA

DNA-citH3 complexes were measured via sandwich ELISA. Briefly, 96-well microtiter plates (Nunc MaxiSorp, ThermoFisher Scientific, Madrid, Spain) were incubated with rabbit anti-citH3 (Abcam, Madrid, Spain) 1:250 in carbonate-bicarbonate buffer pH 9.6 overnight at 4°C. Blocking was performed by incubation with 200 µL PBS 5% BSA. Wells were rinsed with wash buffer (PBS 1% BSA 0.05% Tween-20), and 50µL of plasma samples were added to wells and incubated for 2h at RT. Wells were washed and incubated with peroxidase-conjugated anti-DNA antibody (Cell Death Detection ELISA Kit, Roche Applied Science, Indianapolis, IN) diluted 1:100 in incubation buffer for 2h at RT. After thorough washing 1-Step ABTS reagent

(ThermoFisher, Madrid, Spain) was added to each well, and the plate was incubated for 2h at RT. The optical density (OD) at 405 nm and 490 nm wavelengths was measured in a plate reader (Biotek® Sinergy TM Ht, Winooski, VT)., and the difference between the two optical densities (OD405-OD490) was used to report relative differences in citH3-DNA complexes abundance.

Video legends

Video S1. Confocal microscopy 3-D movie providing a 360° rotation of a neutrophil. Spatial distribution of DNA (DAPI, blue), NE (green), and H2B (red) in one neutrophil found in an atheroma plate of aortic root from a WT BM transplanted *Ldlr*^{-/-} mouse. Z-stacks captured with a Leica TCS SP8 confocal microscope where reconstructed using the LASAF 3D Viewer Module.

Video S2. Confocal microscopy 3-D movie providing a 360° rotation of a NET. Spatial distribution of DNA (DAPI, blue), NE (green), and H2B (red) in a NET found in an atheroma plate of aortic root from a *miR-146a*^{-/-} BM transplanted *Ldlr*^{-/-} mouse. Z-stacks captured with a Leica TCS SP8 confocal microscope where reconstructed using the LASAF 3D Viewer Module.

References

1. Schneider CA, Rasband WS, Eliceiri KW. NIH Image to ImageJ: 25 years of image analysis. *Nat Methods* 2012;9(7):671–675.
2. Schindelin J, Arganda-Carreras I, Frise E, Kaynig V, Longair M, Pietzsch T, Preibisch S, Rueden C, Saalfeld S, Schmid B, Tinevez J-Y, White DJ, Hartenstein V, Eliceiri K, Tomancak P, Cardona A. Fiji: an open-source platform for biological-image analysis. *Nat Methods* 2012;9(7):676–682.
3. Brinkmann V, Abed UA, Goosmann C, Zychlinsky A. Immunodetection of NETs in paraffin-embedded tissue. *Front Immunol* 2016;7:513.
4. Fine MJ, Auble TE, Yealy DM, Hanusa BH, Weissfeld LA, Singer DE, Coley CM, Marrie TJ, Kapoor WN. A Prediction Rule to Identify Low-Risk Patients with Community-Acquired Pneumonia. *N Engl J Med* 1997;336(4):243–250.
5. Singer M, Deutschman CS, Seymour CW, Shankar-Hari M, Annane D, Bauer M, Bellomo R, Bernard GR, Chiche J-D, Coopersmith CM, Hotchkiss RS, Levy MM, Marshall JC, Martin GS, Opal SM, Rubenfeld GD, van der Poll T, Vincent J-L, Angus DC. The Third International Consensus Definitions for Sepsis and Septic Shock (Sepsis-3). *JAMA* 2016;315(8):801-810
6. Vincent JL, de Mendonça A, Cantraine F, Moreno R, Takala J, Suter PM, Sprung CL, Colardyn F, Blecher S. Use of the SOFA score to assess the incidence of organ dysfunction/failure in intensive care units: results of a multicenter, prospective study. Working group on "sepsis-related problems" of the European Society of Intensive Care

Medicine. Crit Care Med 1998;26(11):1793–800.

7. Menendez R, Torres A, Rodriguez de Castro F, Zalacain R, Aspa J, Martin Villasclaras JJ, Borderias L, Benitez JMM, Ruiz-Manzano J, Blanquer J, Perez D, Puzo C, Sanchez-Gascon F, Gallardo J, Alvarez CJ, Molinos L, Neumofail Group. Reaching Stability in Community-Acquired Pneumonia: The Effects of the Severity of Disease, Treatment, and the Characteristics of Patients. Clin Infect Dis 2004;39(12):1783–1790.
8. Menendez R, Cavalcanti M, Reyes S, Mensa J, Martinez R, Marcos MA, Filella X, Niederman M, Torres A. Markers of treatment failure in hospitalised community acquired pneumonia. Thorax 2008;63(5):447–452.
9. Menéndez R, Méndez R, Aldás I, Reyes S, Gonzalez-Jimenez P, España PP, Almirall J, Alonso R, Suescun M, Martinez-Dolz L, Torres A. Community-Acquired Pneumonia Patients at-risk for Early and Long-term Cardiovascular Events are Identified by Cardiac Biomarkers. Chest 2019; 156(6):1080-1091.

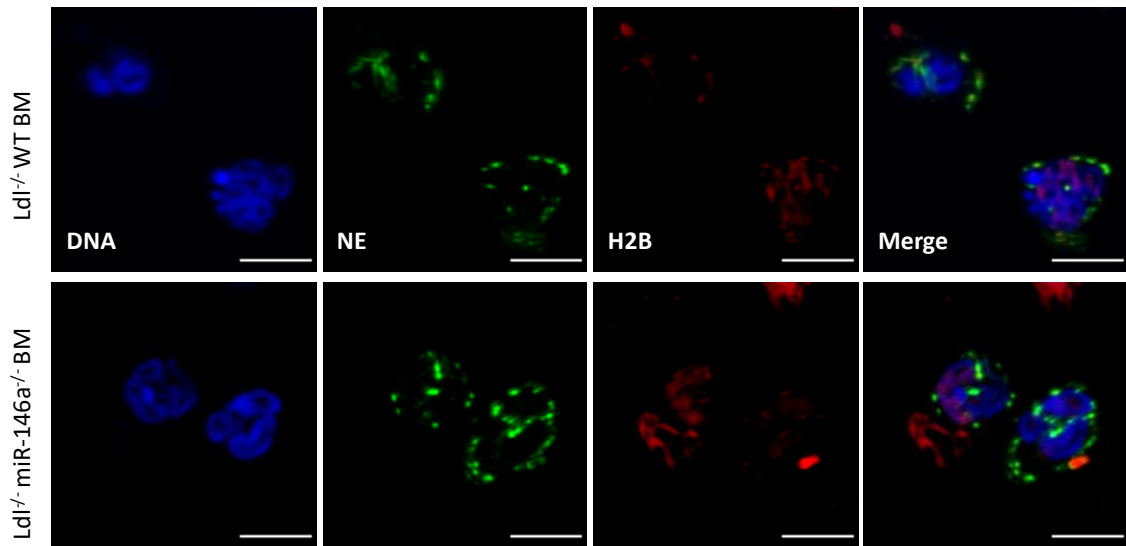


Figure S1. Detail of neutrophils found in aorta sections of WT and *miR-146a*^{-/-} BM transplanted *Ldlr*^{-/-} mice. Images from aortic valve leaflets shown of Figure 1D. Bar represents 5 μ m.

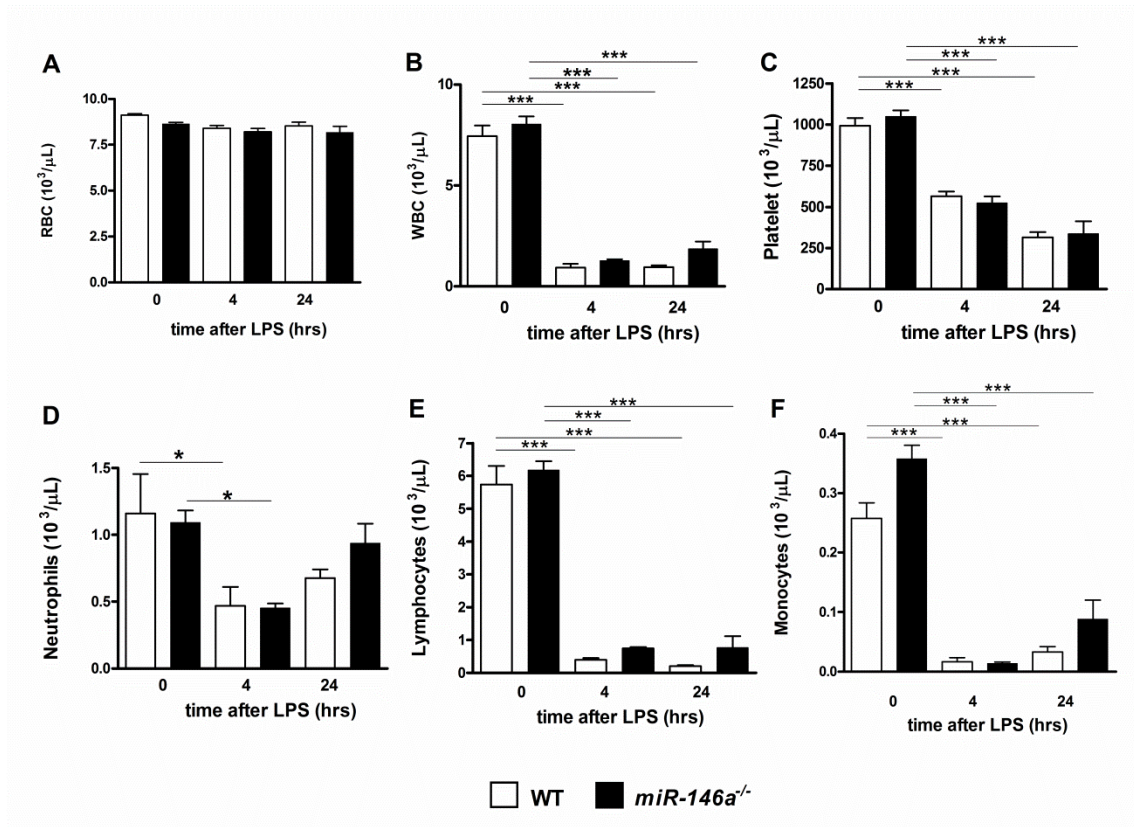


Figure S2. Peripheral blood cells count from WT and *miR-146a*^{-/-} mice after LPS stimulation. Blood was extracted by retro-orbital bleeding and circulating cells were quantified at 0 (n=8-9/group), 4 (n=9-10/group) and 24 h (n=6/group) after LPS treatment (1mg/Kg). (A) Red blood cells (RBC), (B) white blood cells (WBC), (C) platelets, (D) neutrophils, (E) lymphocytes and (F) monocytes. Circulating blood cells were quantified using the PENTRA 80 hematology platform (HORIBA Medical, Madrid, Spain). *P*-value calculations were performed using 1-way ANOVA on ranks with the Bonferroni post hoc test. Data represent mean \pm SEM, * $p < 0.05$, ** $p < 0.01$, *** $p < 0.001$.

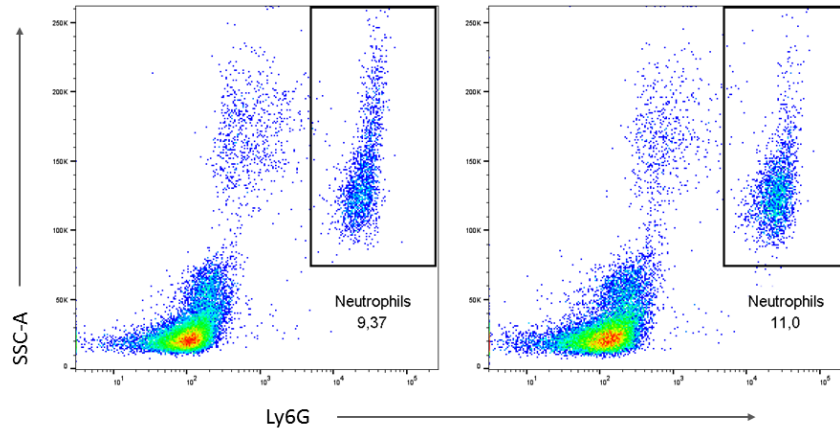


Figure S3. Dot plots showing the identification of neutrophils population selected for further phenotype marker analysis. Neutrophils from WT (left panel) and *miR-146a*^{-/-} (right panel) mice were gated on the basis of their Ly6G-Alexa 647 and side-scatter (SSC-A) profiles.

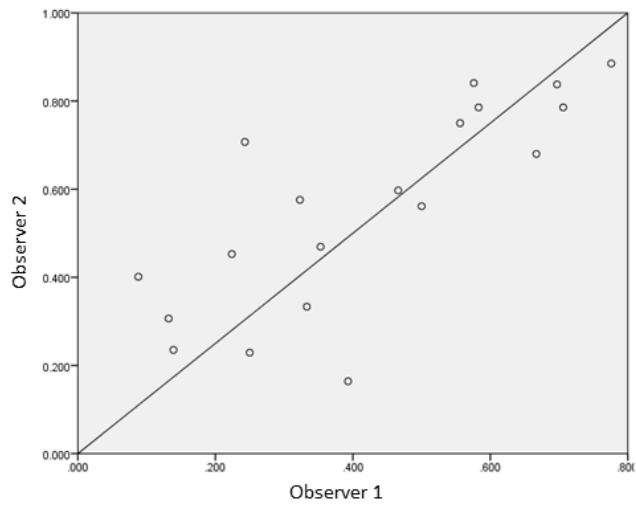


Figure S4. Scatter plot for citH3/total nucleated cell ratio found by two different observers in a blinded fashion for thrombi of carotid sections. Diagonal line represents equality for paired data. Intraclass correlation coefficient (ICC) ranged between 0.81-1, indicating near complete agreement for the two observers (ICC = 0.848; $p < 0.0001$).

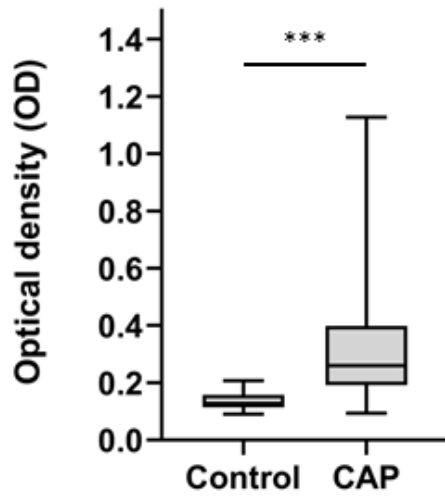


Figure S5. DNA-citH3 plasma complex levels are elevated in CAP patients. CAP patients (N=112) showed significantly higher DNA-citH3 complex levels than control group (N=30) ($p < 0.0001$). Control group maximum DNA-citH3 level (OD=0.200) was used as cut off point for positive NETs in intra CAP group analysis.

Supplemental Table S1. Demographic and clinical characteristics of patients with CAP according to rs2431697 genotype.

	All N (%)	rs2431697			p*
		CC N (%)	CT N (%)	TT N (%)	
Total N (%)	259 (100)	58 (22.4)	109 (42.1)	92 (35.5)	
Age; median (IQ range)	77 (70-84)	76 (67-83)	78 (70-84)	76 (71-83)	0.257
Female; N (%)	86 (33.2)	15 (25.9)	44 (40.4)	27 (29.3)	0.103
Diabetes mellitus	94 (36.3)	25 (43.1)	39 (35.8)	30 (32.6)	0.424
History coronary artery disease	90 (34.7)	16 (27.6)	35 (32.1)	39 (42.4)	0.134
Hypertension	162 (62.5)	39 (68.4)	70 (64.2)	53 (58.2)	0.433
Dyslipidemia	131 (50.6)	28 (48.3)	59 (54.1)	44 (47.8)	0.621
Current smoking	47 (19.3)	15 (26.3)	15 (14.6)	17 (20.5)	0.701
Sepsis; N (%)	160 (61.8)	35 (60.3)	61 (56)	64 (69.6)	0.165
SOFA; media	2.32	2.24	2.18	2.52	0.235
Neutrophil/mL; median (IQ range)	11510 (8328-15569)	11912 (8098-16066)	10975 (8609-13587)	11718 (8223-15755)	0.743

SOFA: Sequential Organ Failure Assessment score

* χ^2 test

Supplemental Table S2. Global comparison of DNA-citH3 levels between healthy controls and CAP patients, and clinical outcomes in patients with high levels of DNA-citH3 (OD \geq 0.200).

	Global			Sepsis			CVE+TF		
	Controls N=30	CAP N=112	p*	Yes N=58	No N=23	p*	Yes N=18	No N=63	p*
DNA-citH3 median OD (IQ range)	0.127 (0.118-0.145)	0.260 (0.230-0.294)	<0.0001	0.373 (0.278-0.498)	0.235 (0.214-0.294)	<0.001	0.447 (0.294-0.528)	0.290 (0.238-0.407)	0.028

CVE: cardiovascular events

TF: Treatment failure

*Mann-Whitney U-test